novamems
SERVICES FOR RELIABILITY

MEMS Switches: status on reliability issues and characterization techniques

Jérémie DHENNIN, F. Coccetti, A. Broué, Nova MEMS
F. Courtade, CNES

ESA round table on MNT
15-18th October 2012

Outline

- Typical failure mechanisms for MEMS switches
- Dielectric charging processes
  - ✓ Modelling
  - ✓ Characterization through KPFM
- Micro contact degradation
  - ✓ Modelling
  - ✓ Characteriztaion through micro-bending tests
- Packaging

Sandia failure mechanisms

Product	Class	Mechanical Wear	Fracture	Fatigue	Optical Degradation (Use)	Charging	Shock	Vibration	Dielectric Breakdown	Change in Friction	Radiation	Thermal Degradation	Thermal Cycling	Humidity	Shock	Vibration	Stress-corrosion cracking	Creep	Environmental Degradation	Optical Degradation	Stiction
DNA Sequencers	I																		x		
Microfluidics (electrostatic)	I								x										x		
Nozzles	I																		x		
Chemical Sensor	I										x								x		
Accelerometer	I or II	x	x	x		x	m	m		x	x			x	x	x		x			x
Pressure Sensor	II		x	x			x	x				x	x					x	x		
Gyro	II					x	x	x			x			x	x	x					
Microfluidic Pumps (Flex)	II		x	x			x	x							x	x	x	x	x		x
Waveguide Switch	II		x	x			x	x						x	x	x	x	x	x		x
Thermal Actuator	III	x					x	x				x	x		x	x					x
Valves	III	x	x	x			x	x				x	x		x	x	x		x		x
Microrelays	III	x	x	x		x	x	x	x	x				x	x	x	x	x			x
Electrostatic Actuator	IV	x	x	x			x	x		x				x	x	x	x	x			x
Optical Shutter	IV	x	x	x			x	x				x	x	x	x	x					x
Mirror Device	IV	x	x	x	x		x	x				x	x	x	x	x				x	
Microfluidic Pumps (Rubbing)	IV	x	x	x			x	x		x					x	x	x		x		x
Geared Devices	IV	x	x	x			x	x		x		x	x	x	x	x	x	x	x		
Microturbine/Fan	IV	x					x	x		x		x	x		x	x	x	x	x		

Failure of micro switches

Fatigue & creep of movable parts

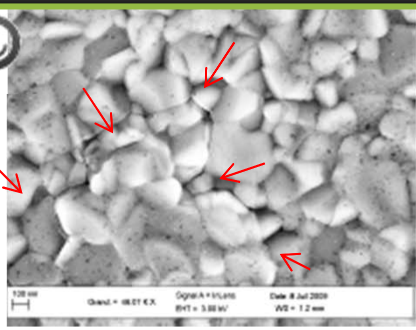

Decohesion of grain boundaries

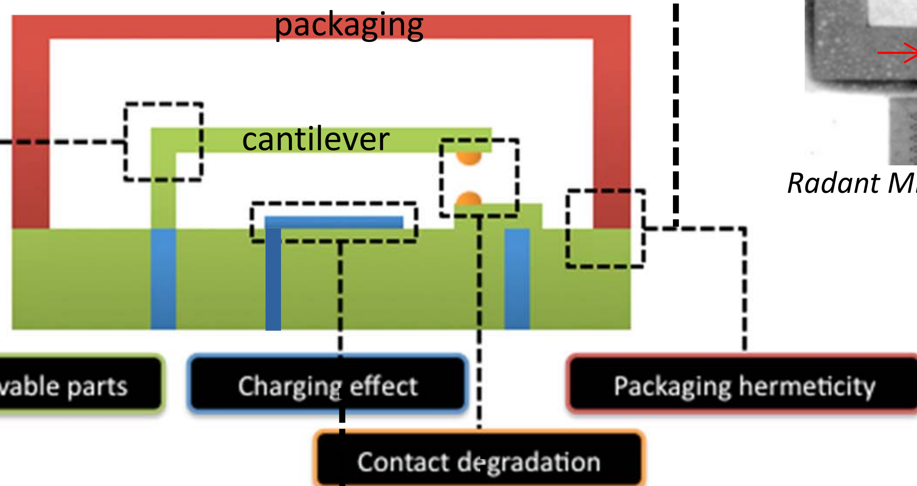

Packaging hermeticity

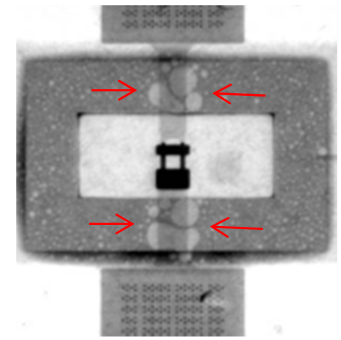

Radant MEMS sealing ring

Charging effect

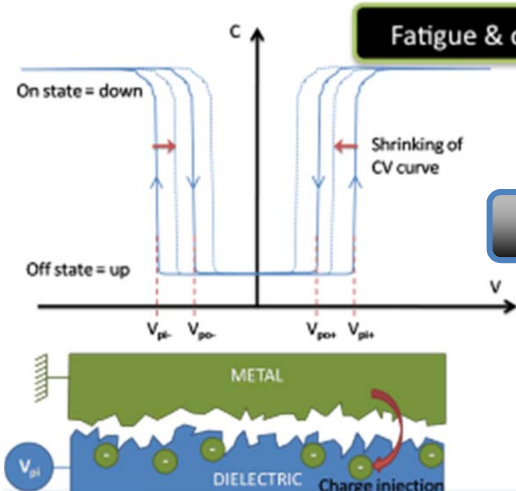

Contact degradation

Material transfers

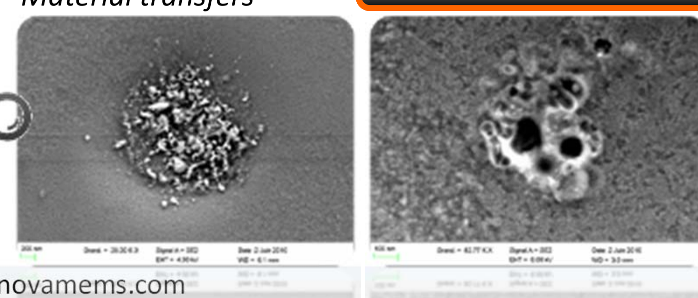

Reliability Modeling of dielectric charging

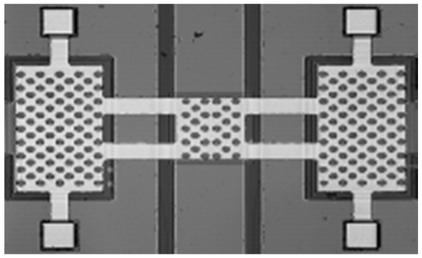

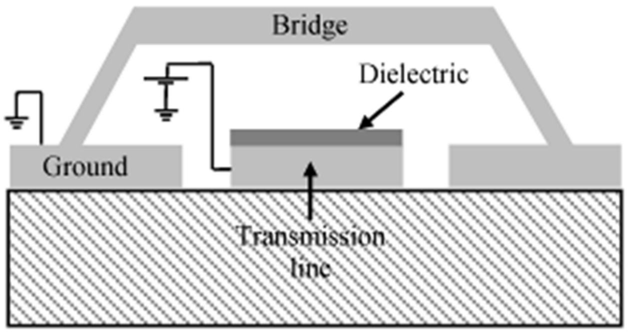

Dielectric charging phenomenon

High electric field across the dielectric

Built-in charges inside the dielectric

Shift in pull-in and pull-out voltages

Fail to open (Stiction) or to close

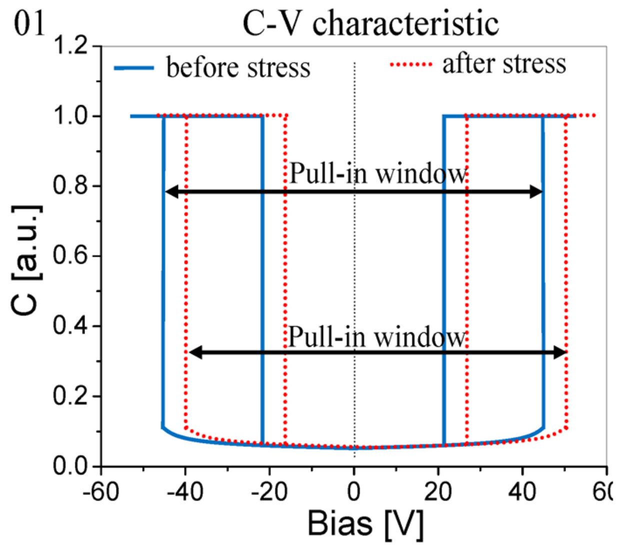

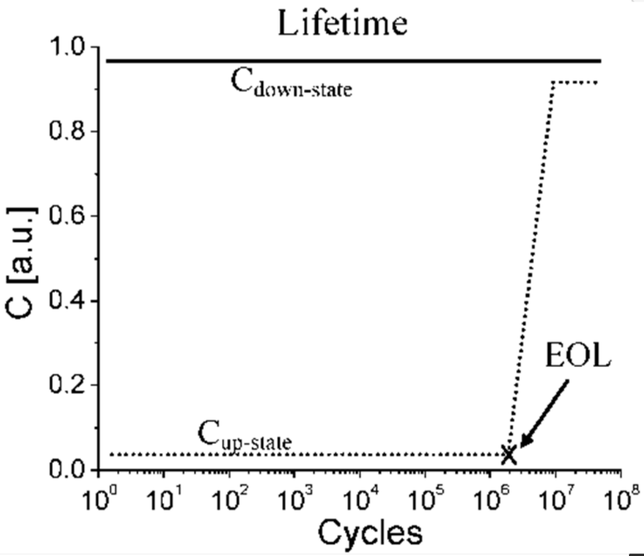

Polynoe program, EDA funding; 2008-2011

Charging effect modelling

Three assumptions must be considered:

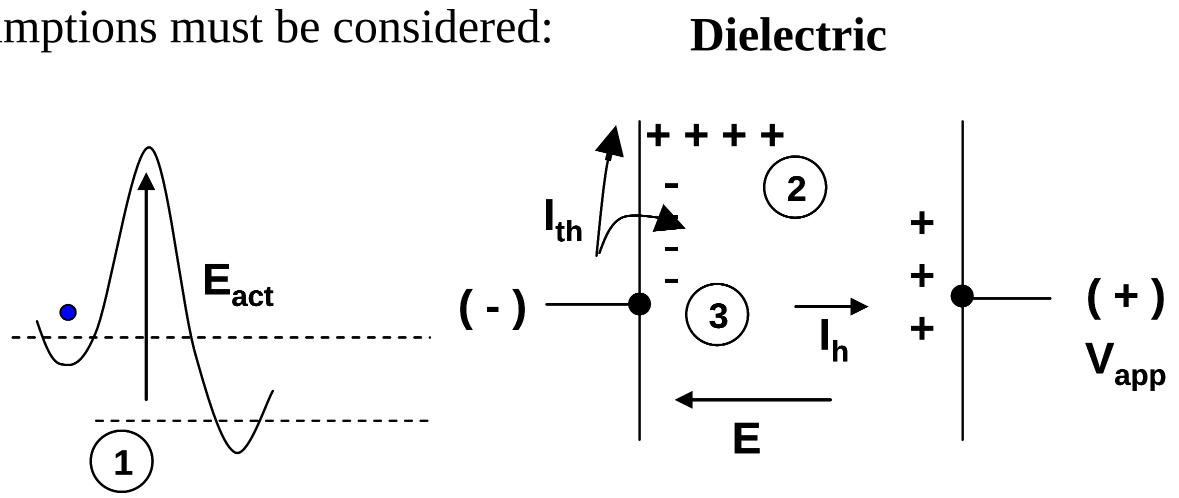

(1) First assumption: Slow polarization effect.

(2) Second assumption: Electrical current passing from site to site.

(3) Third assumption: Direct exchange due to the tunnel effect.

The possible mechanisms of charging effects

Charging effect modelling

In an equivalent electrical model, the slow polarization phenomena in this dielectric material can be presented by two capacitance Co and Cv, placed in parallel where:

$$C_0 = \frac{\varepsilon_r * A}{t} \qquad C_v(t) = \varepsilon(t) * \frac{A}{t}$$

t : Thickness.

A : Area.

ε_r **: Dielectric constant.**

$\varepsilon(t)$ **: time evolution of the dielectric constant.**

$$V_{Shift} = V_2 - V_1 = \frac{-C_a C_v}{(C_0 + C_v)(C_0 + C_a)} V_{actuation\,(pull-in)\,(pull-out)}$$

Ideal case

Case with charging Effect

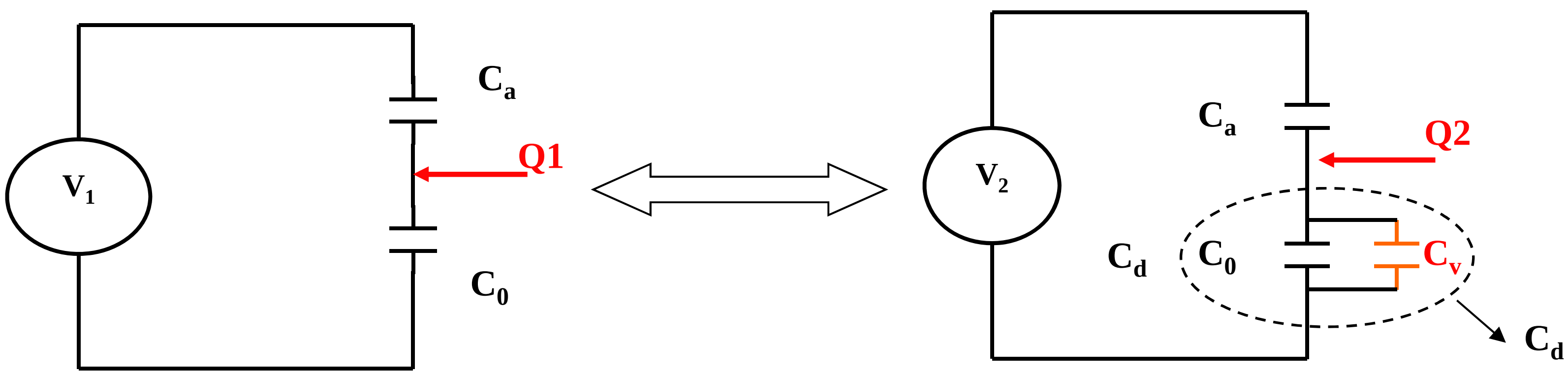

Capacitance and drift voltage variation

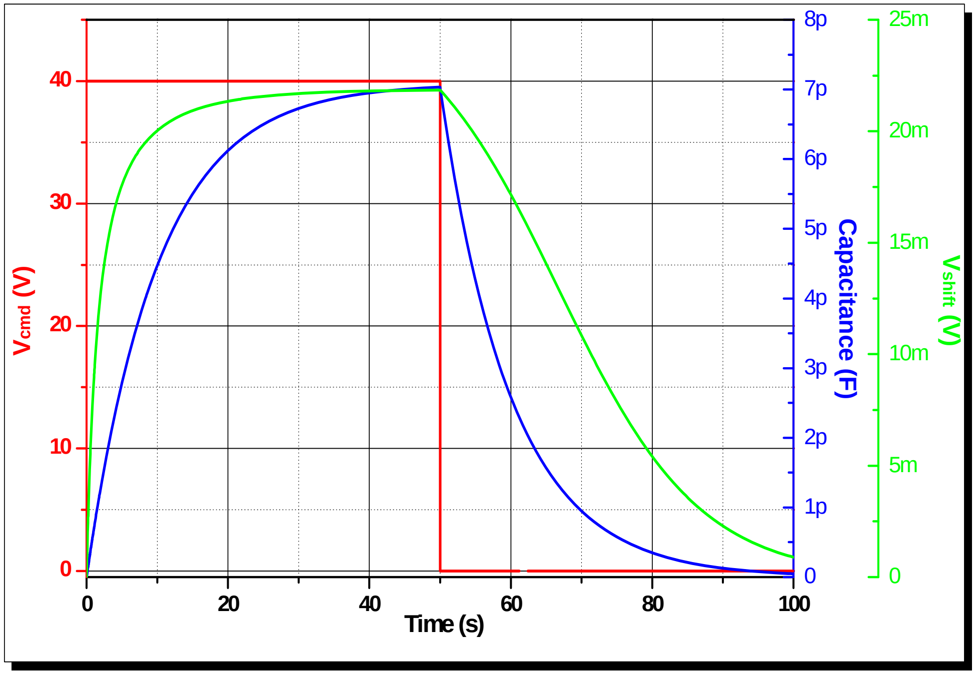

Bias voltage

$$C_v(t) = \varepsilon(t) * \frac{A}{t}$$

$$\varepsilon_f = \alpha * V_f$$

$$\frac{\partial \varepsilon}{\partial t} = \frac{\varepsilon_f - \varepsilon}{\tau}$$

$$V_{Shift} = \frac{-C_a C_v}{(C_0 + C_v)(C_0 + C_a)} V_{actuation\,(pull-in)\,(pull-out)}$$

Reliability model implemented in VHDL-AMS

VHDL-AMS results: drift voltage for different applied voltage amplitudes

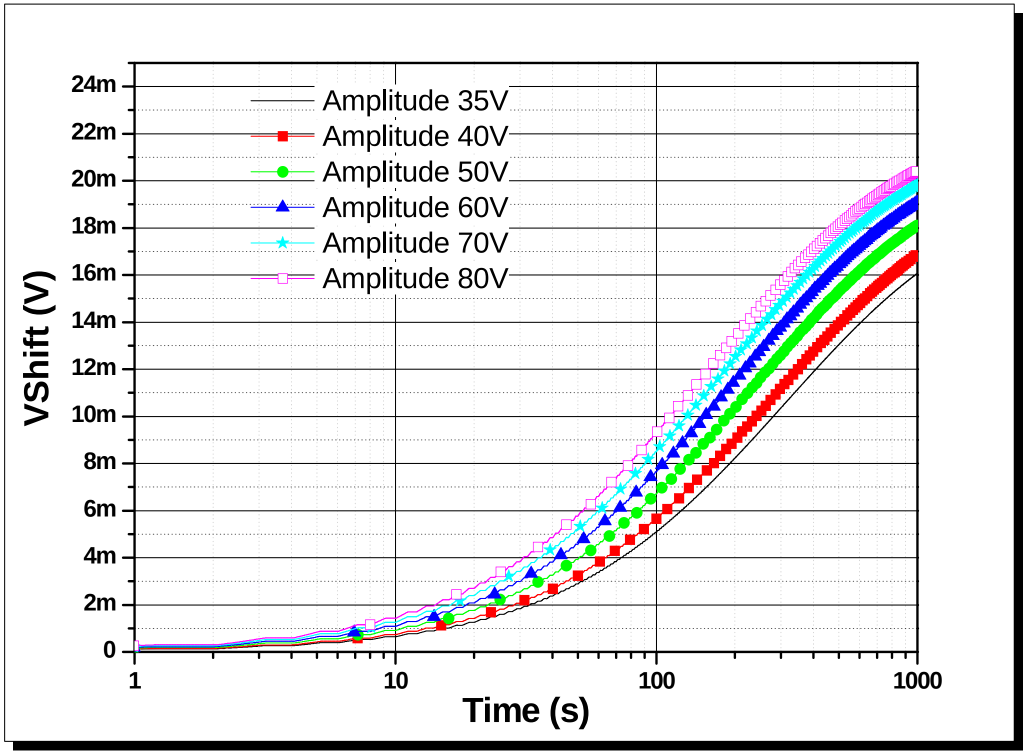

M. Matmat et al ESREF 2010

As the amplitude increases, the drift voltage increases

Experimental reliability tests:
Kelvin Probe Force Microscopy techniques

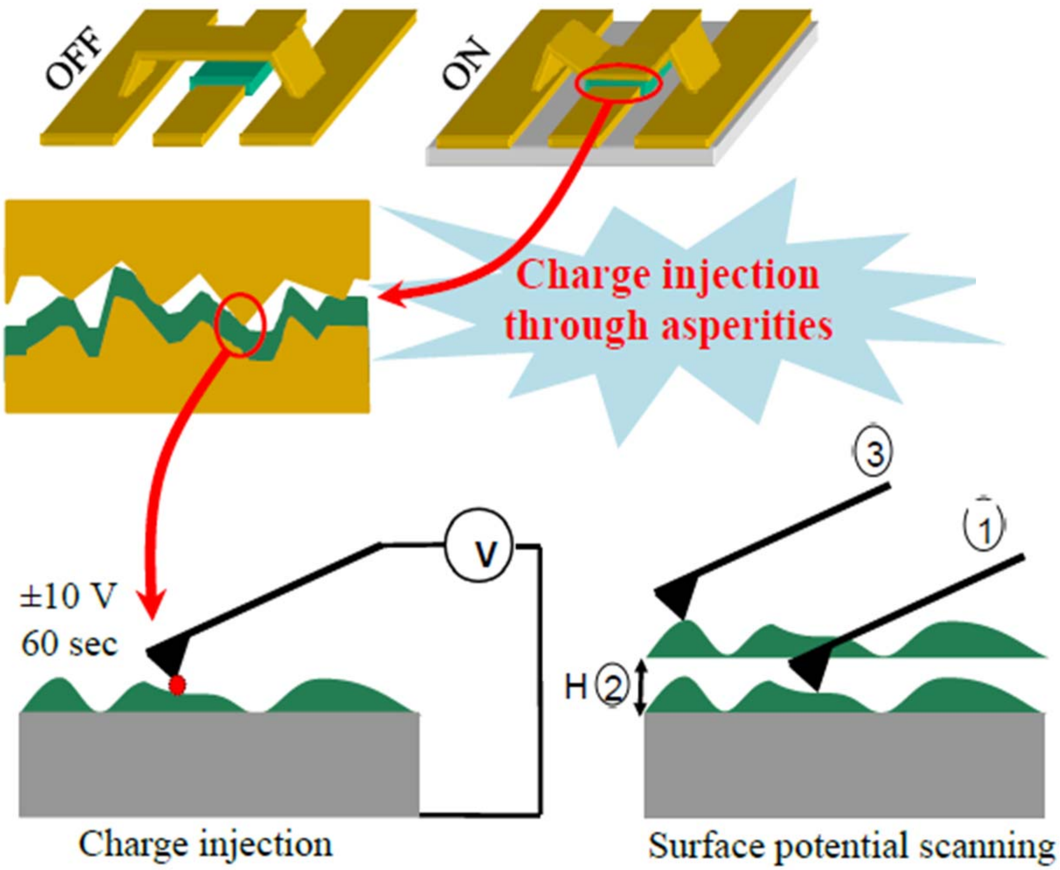

Methodology: Using KPFM to simulate charge injection through asperities

- **Understand** charging/discharging processes on the nanoscale (single asperity level)
- **Low-cost** technique (bare dielectric films)

Experimental reliability tests:
Kelvin Probe Force Microscopy techniques

Charge injection in tapping mode

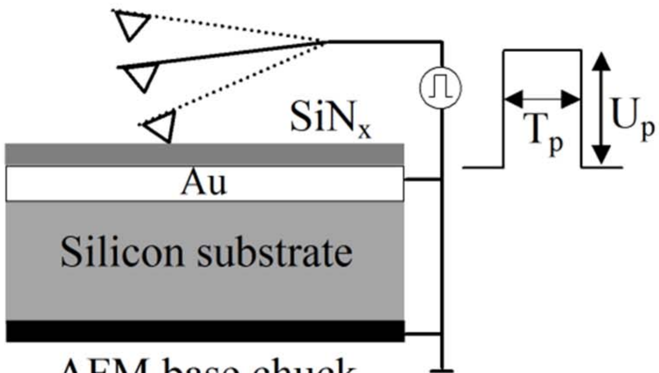

(a)

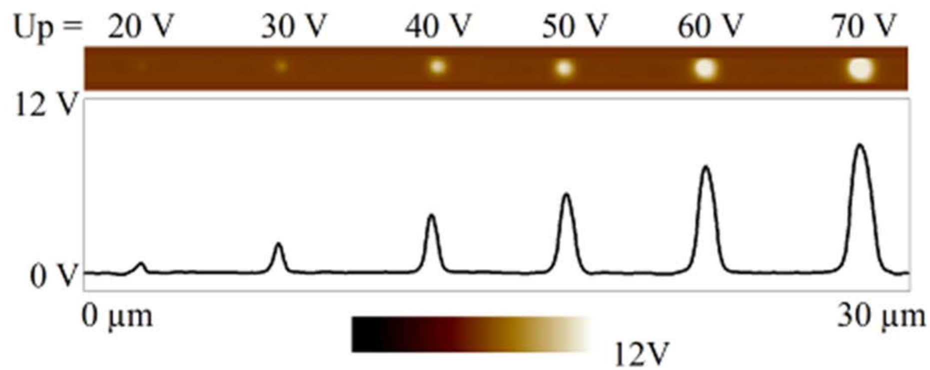

Induced surface potential

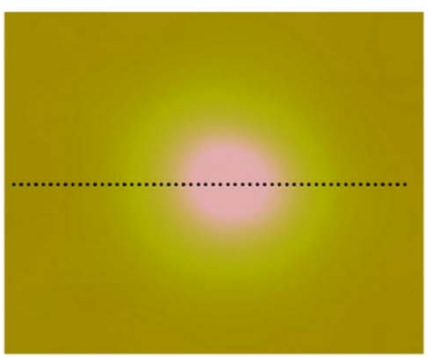

(b)

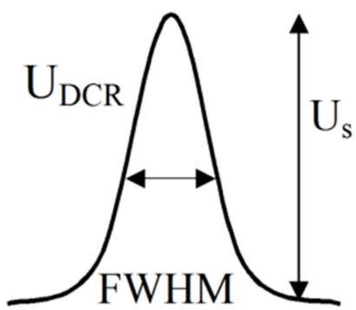

(c)

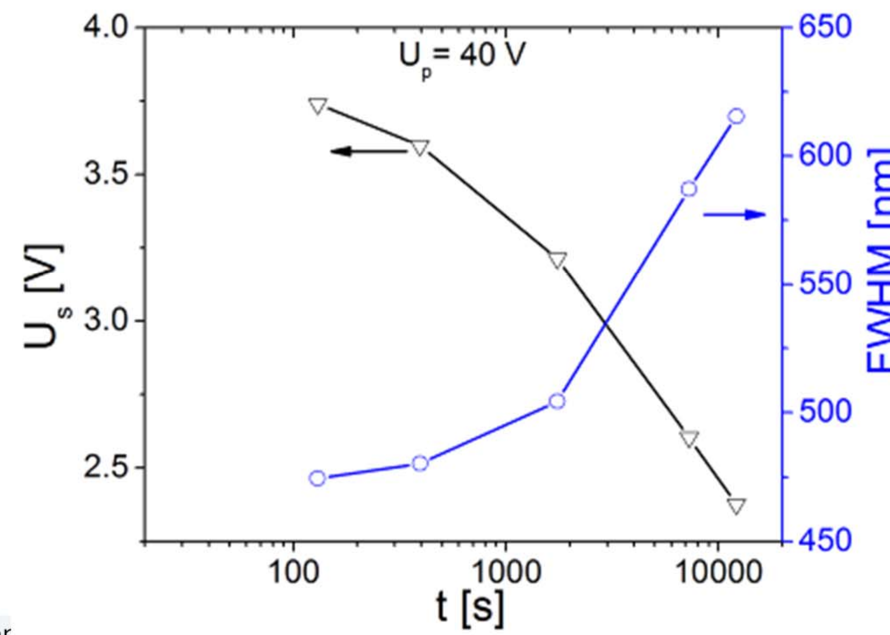

Experimental reliability tests:
Kelvin Probe Force Microscopy techniques

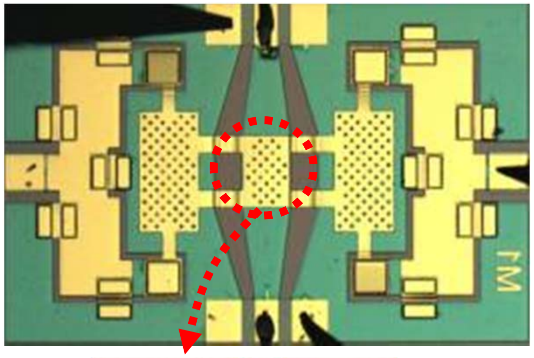

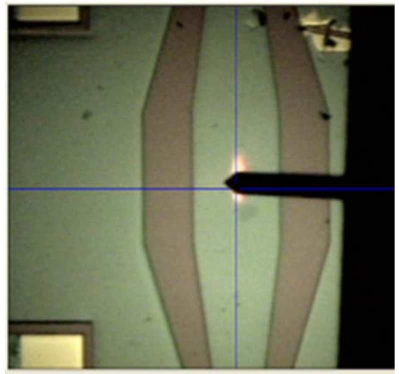

During KPFM scanning

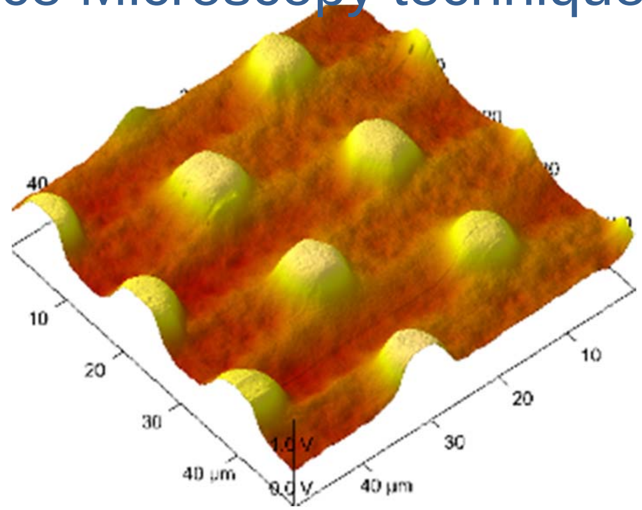

Microscope picture

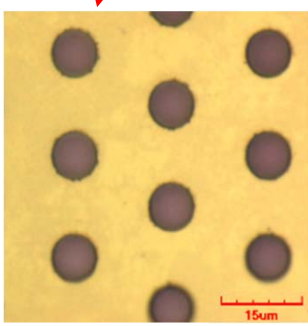

Surface potential

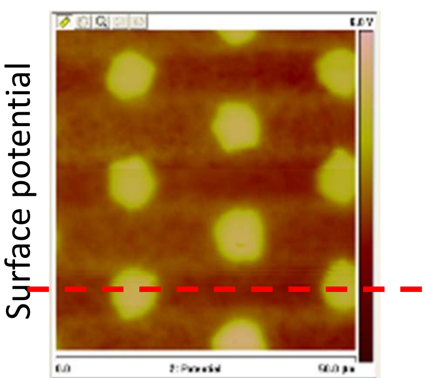

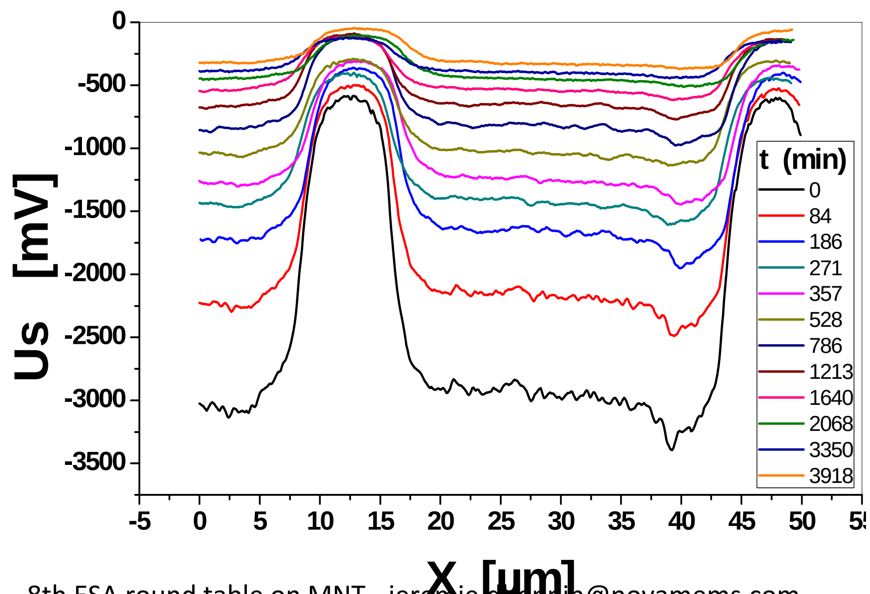

U. Zaghloul et al., *J. Microelec. Reliab.*, 2010

U. Zaghloul et al., *J. Vacuum Science and Technology (in press)*, 2011

Influence of relative humidity on dielectric charging

Results from the KPFM investigations

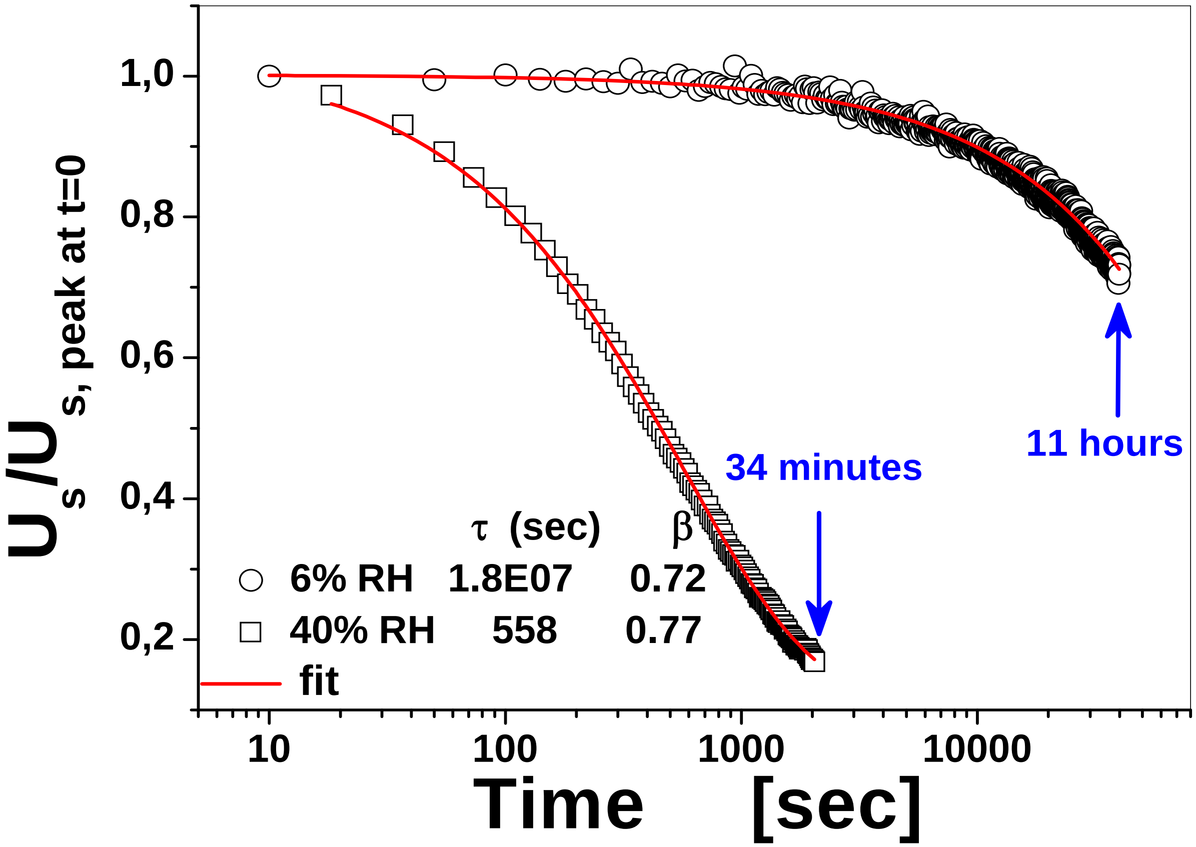

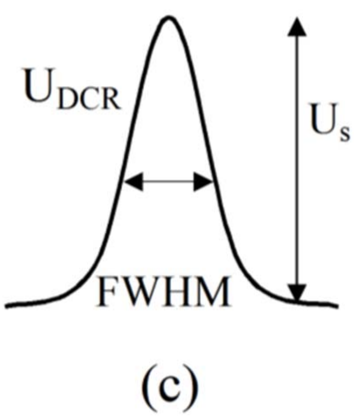

Influence of environment gases and relative humidity

High Humidity →

+ Faster charging/discharging
+ Lower surface potential
- **Wider surface potential**
- **Higher background potential**

$\sum$ **Higher overal potential (i.e. charging)**

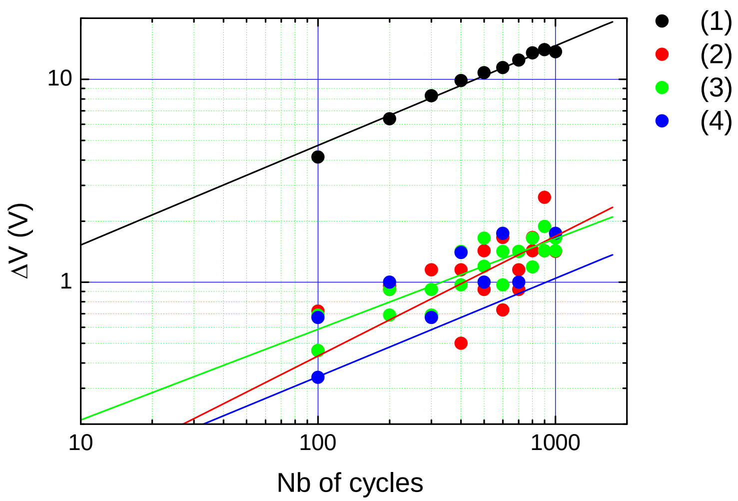

1: Room conditions @ ~296K, 45% RH
2: Vacuum @ 1.4E-5 mbar – 296K
3: N2 @ 1.02 atm – 296K
4: Vacuum @ 2.2E-6 mbar – 223K

Nanotechnology **22 (2011) 035705 U Zaghloul *et al***

Micro contact failure

- OMRON Switch:
  - ✓ « Contact sticking during "**hot switching**" was the major design issue that needed to be resolved. Contact geometry and a proprietary metallurgical alloy were the keys to success. »

FAME program, ANR funding, 2008-2011

Micro-contact reliability
Failure mechanisms

- Commonly reported failure mechanisms are:

- Mechanical (cold welding, strain hardening, wear, fretting…)
- Electro-thermal (hot welding, annealing, arcing, creep, softening…)
- Chemical (contaminations, frictional polymers, corrosion, oxidation or sulfidation: formation of insulating films at the extreme surface)

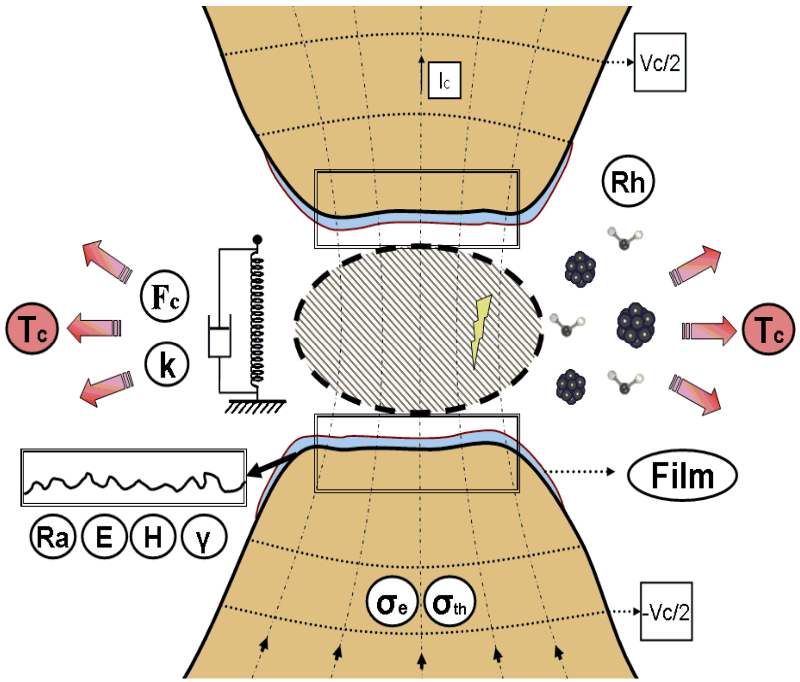

▪ All inducing modifications of the topological, mechanical and/or electrical properties of the contact

Micro-contact physics

The effective contact area is largely **smaller** than the apparent one ➔ due to the **small force** available in micro actuators (50 – 250 µN)

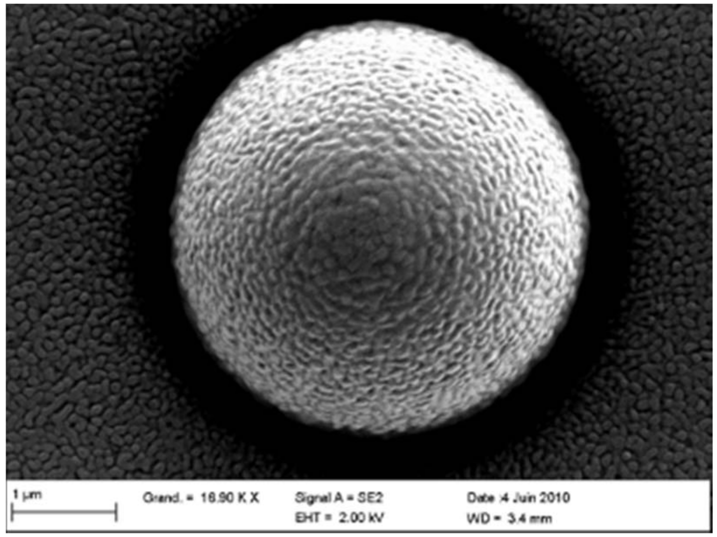

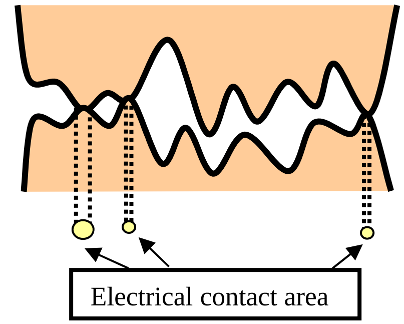

- The contact resistance *Rc* is linked to the constriction of current lines between both contacts ➔ local increase of the current density + ballistic transport of electrons

/!\ breakdown of classical theory

$$R_{Contact} = \underbrace{\Gamma(K) R_{Holm}}_{\text{Diffusive}} + \underbrace{R_{Sharvin}}_{\text{Ballistic}} \left(+R_{Film}\,?\right)$$

where $R_{Holm} = \dfrac{\rho}{2a}$ and $R_{Sharvin} = \dfrac{4\rho K}{3\pi a}$

Relationship between contact resistance *Rc* and the load applied *Fc* on the contact

$$R_C = A F_C^{-x}$$

The highest contact spot temperature T_c expressed as a function of the contact voltage V_c

$$T_c = \sqrt{\frac{V_c^{\,2}}{4L} + T_0}$$

Micro-contact physics
Contact temperature focus

» Plastic deformation proceeds more rapidly when the softening temperature of the contact material is reached → Softening of the contact metal reduces the strain hardening of the asperities

→ The effective contact area increases inducing a drop of the contact resistance

→ It could accelerate aging of the contact by the activation of thermal failure mechanisms (material transfers, modification of the contact surfaces, adhesion …)

» Temperature also controls mechanisms such as oxidation, corrosion, or creep

Contact temperature is a first order parameter

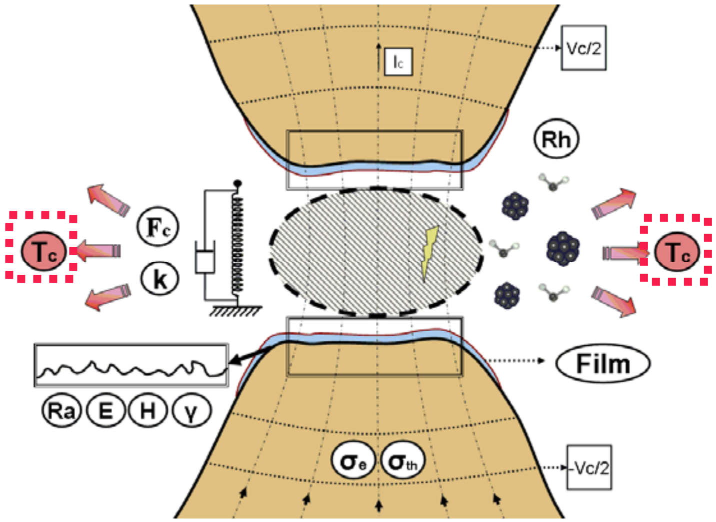

*The contact is heated by Joule effect

Description of the experimental set-up

- Specific contact investigation:

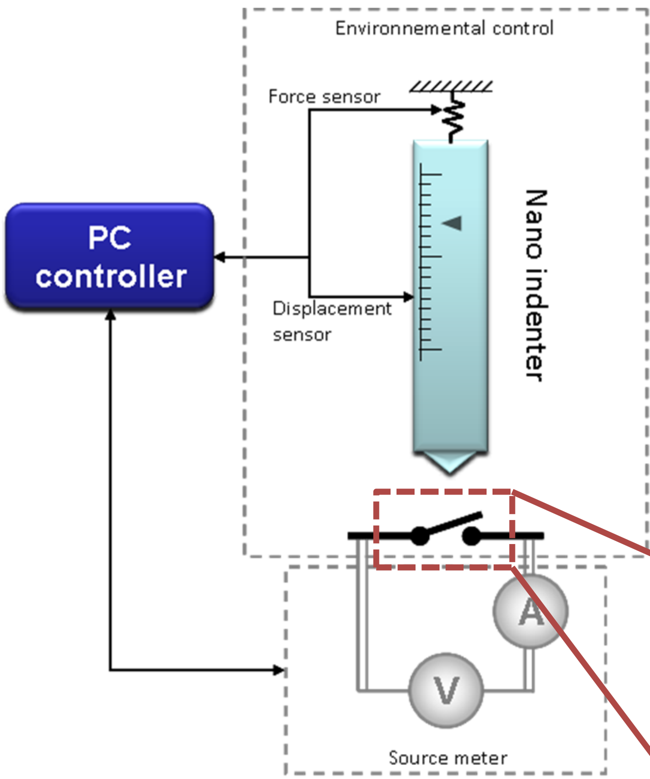

Source Modes	Switching Modes
•Current source or voltage source	Hot switching Cold switching Mechanical switching
Input Parameters	**Range**
•Current level (Ic)	10^{-5} to 1A
•Maximum load applied (L_{max})	1µN to 6mN
•Contact voltage(Uc)	10^{-5} to 40V
•Holding plateau at load max t_{hold}	0 to several min
Environment	Dry nitrogen (< 5% RH)
Outputs	
•Voltage Drop (Vc) or current drop (Ic) [depending on the source mode]	•Contact stiffness (K)
	•Contact resistance (Rc)

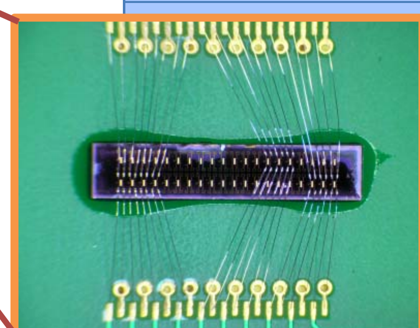

*Contact force resolution = 1µN
displacement resolution = 1nm

*test structures are reported and micro bonded on a PCB (Printed Circuit Board).

Test vehicle description

- LETI specimens (same method for measuring contact resistance as the one used in crossed rod design of Holm)

Side view

Top view

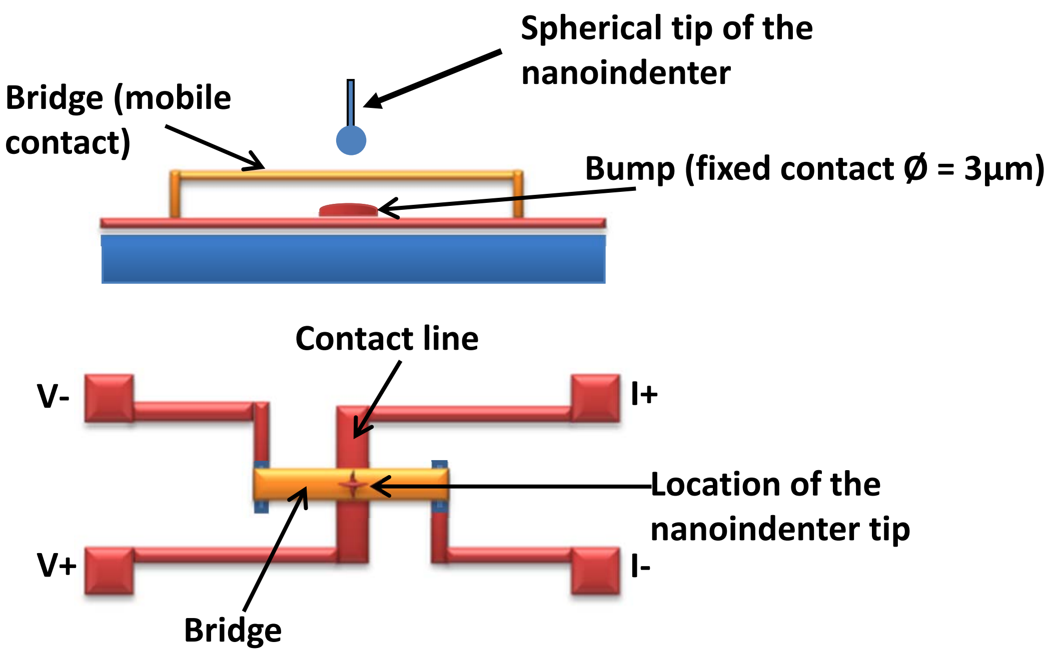

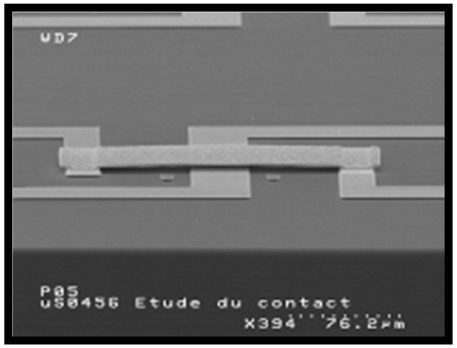

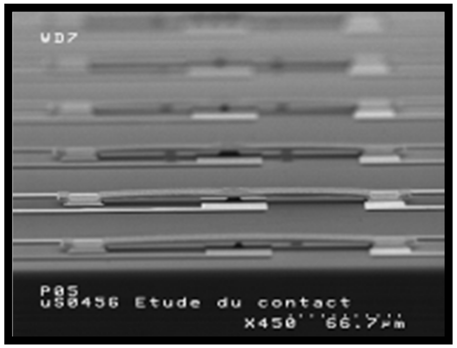

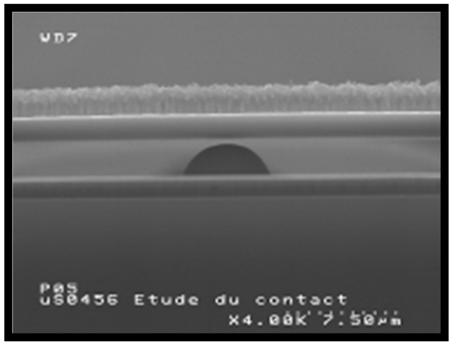

*stored in dry N2 to slow down any environmental contamination of the contact surfaces, but gradual contamination accumulation still occurred

Results: R_C VS F_C

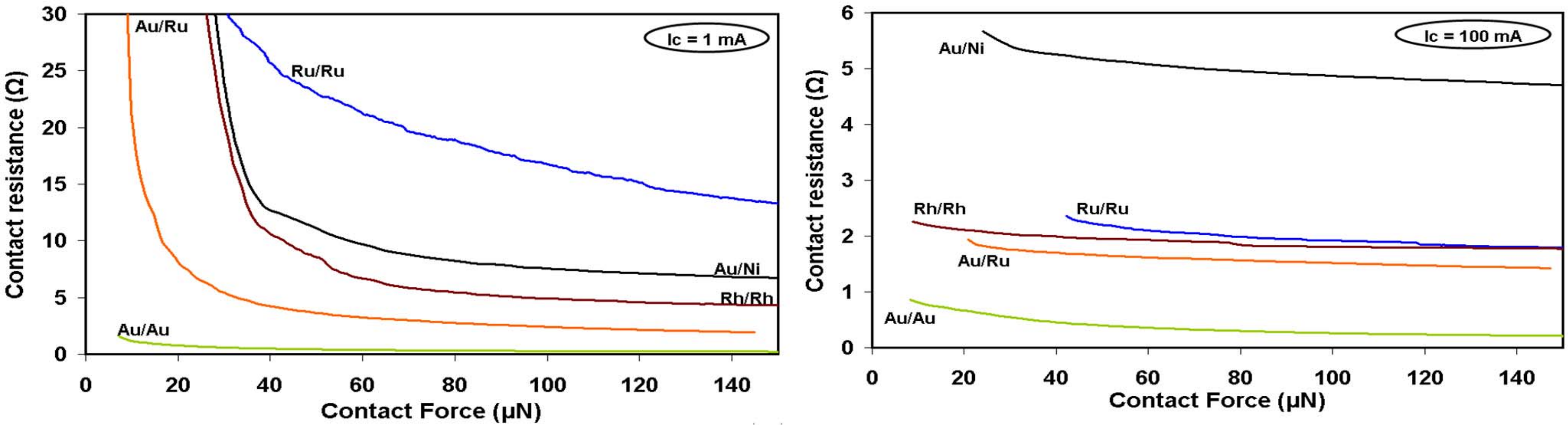

Contact resistance versus contact force as a function of the current flowing through the contact for Au/Ru, Au/Au, Ru/Ru, Rh/Rh and Au/Ni contacts at 1mA and 100mA ($V_{compliance}$ = 1V)

- **Au/Au contact** shows the more stable and the lowest contact resistance beyond contact force about 40µN from 1mA (R_c = 0.49Ω) to 100mA (R_c = 0.45Ω)
- **Rh/Rh contact** reaches a lower contact resistance at 140µN compared to the **Ru/Ru contact** at 1mA. This result could be attributed to the low resistivity of the rhodium compared to the ruthenium.
- **Au/Ru bimetallic contact** is relatively stable at the maximum contact load. From 1mA to 100mA, the contact resistance at 145µN decreases from 1.9Ω to 1.4Ω.

Results: Contact heating focus

> Monometallic contacts

- ✓ *Tc* increases until reaching the softening temperature
- ✓ From the softening temperature, the *Tc* stops to increase and it seems to oscillate around the softening temperature.
- ✓ Softening temperature for Rhodium is **~360°C** (unknown in literature)

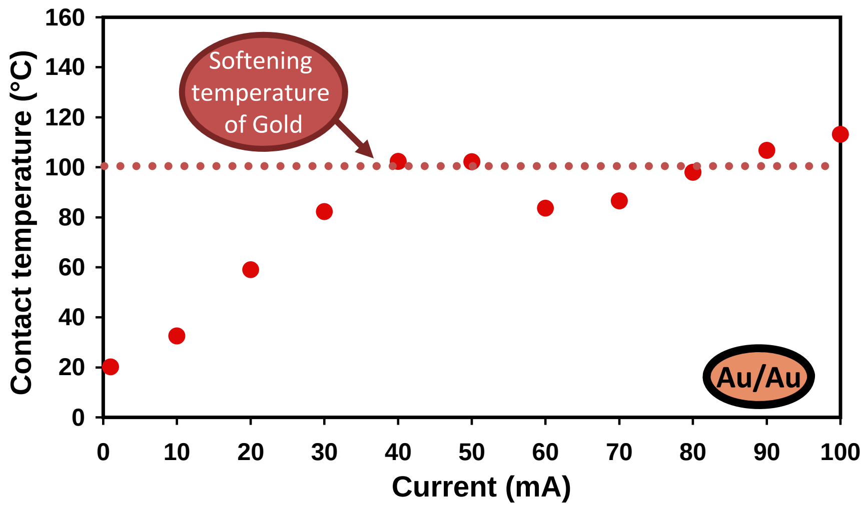

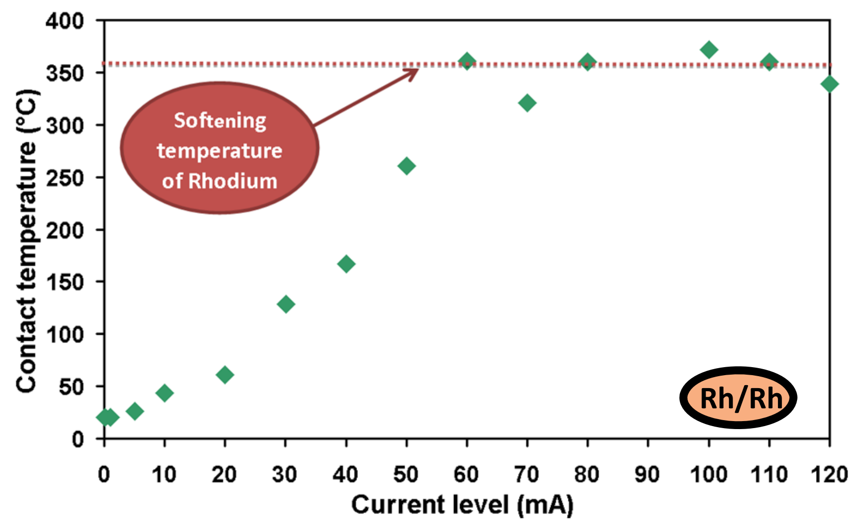

Results: Contact heating focus

> Bimetallic contacts

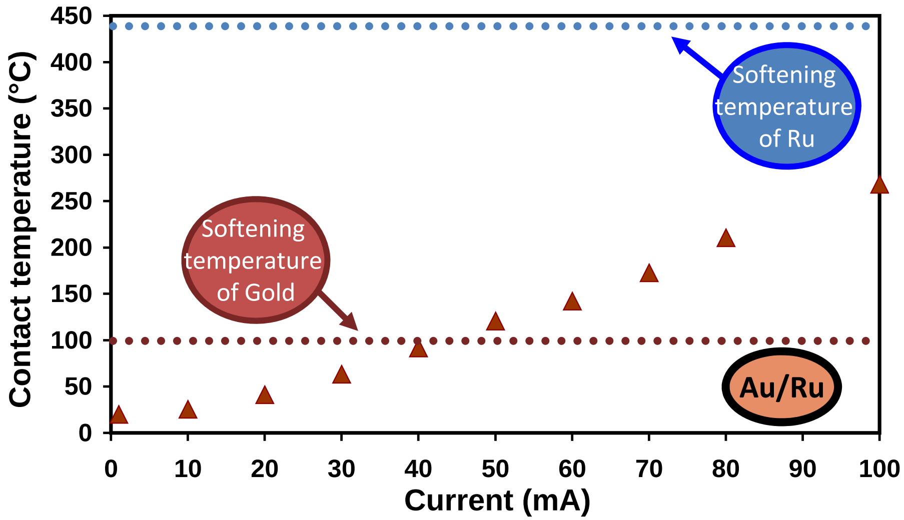

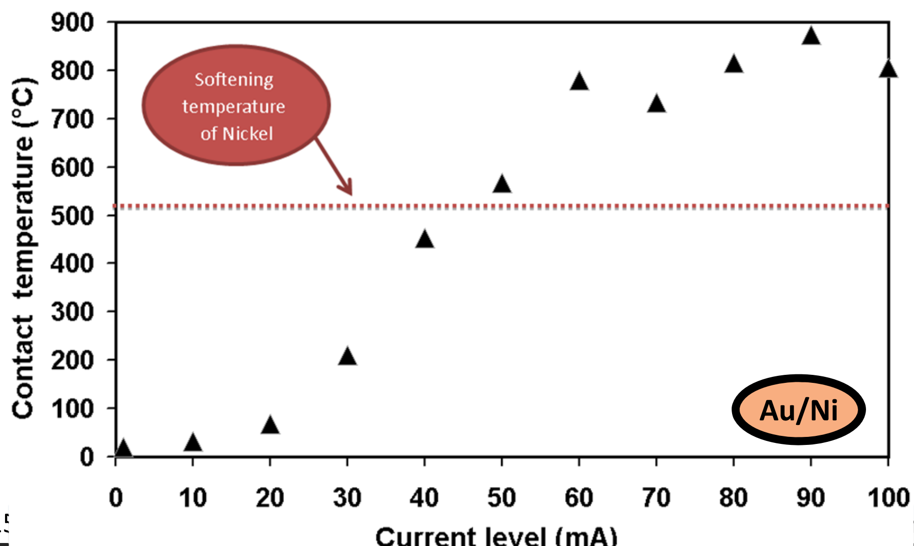

- » Tc increases without reaching a maximum for **Au/Ru contact**
- » The leveling of the potentials across the **Au/Ni contact** is observed, but for contact temperatures largely higher than the nickel or the gold softening temperature
- » The behavior is different in comparison with monometallic contacts

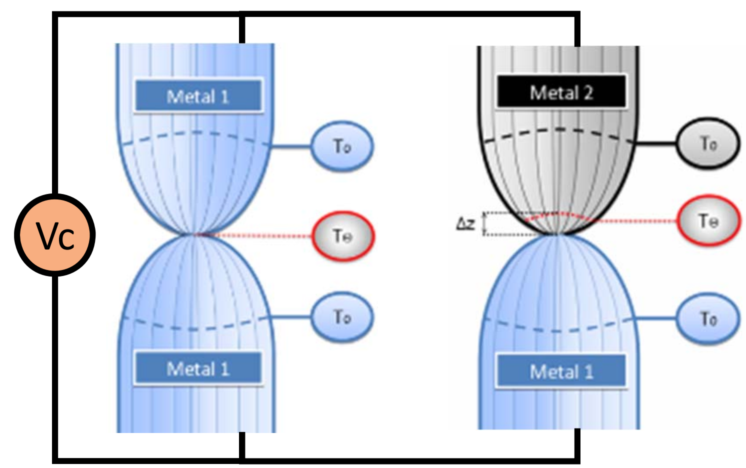

Wafer level packaging

- MEMSPACK FP7 project (IMEC lead) 2009-2011

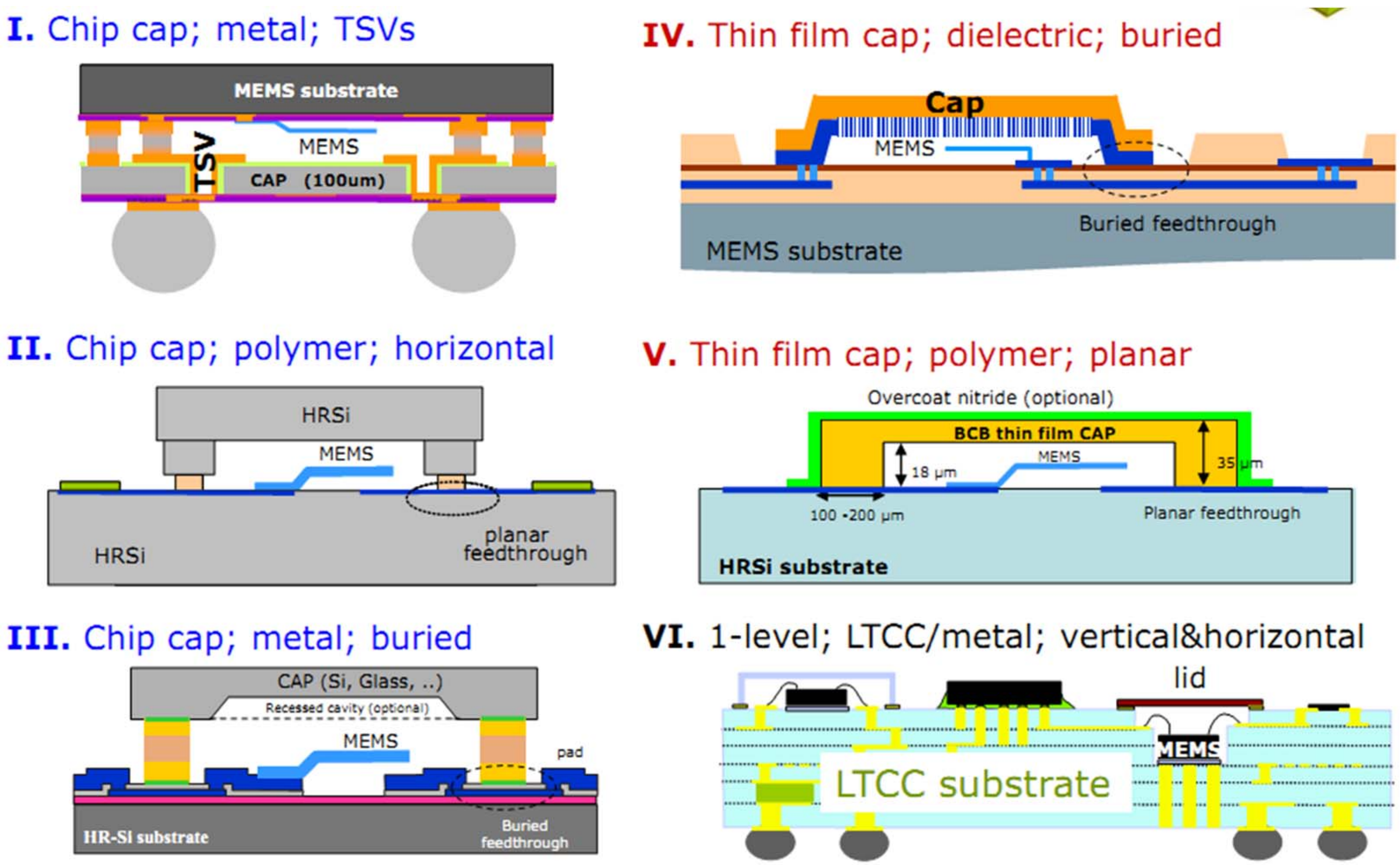

Packaging assessment

- Advanced hermeticity determination

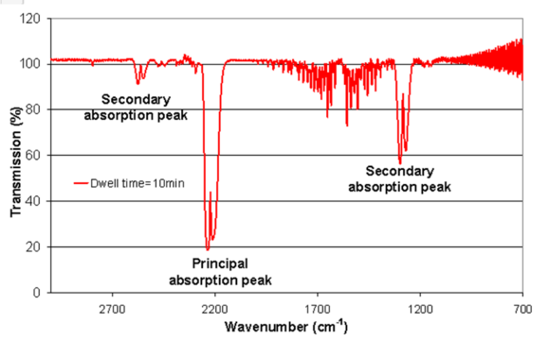

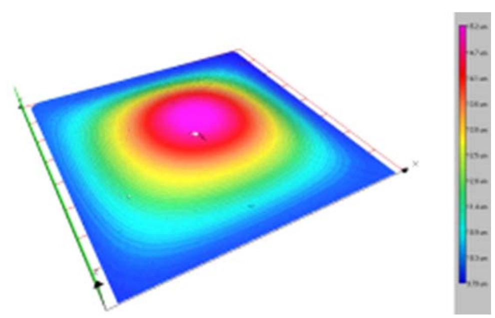

He Absorption (MIL-STD 883)

- He pressurization
- Dwell time
- Mass spectroscopy of the gases escaping the cavity

N_2O Absorption (FT-IR)

- Transmission measurement (reference)
- N_2O pressurization
- Dwell time
- Transmission measurement(sample)

Membrane deflection

- Initial deflection measurement
- He Pressurization
- Final deflection measurement

D. Lellouchi et al.
JMM 2010

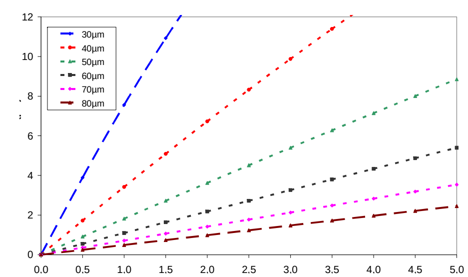

Déflexion = f(Pressure)

…